



20 **Abstract**

21 Soil organic carbon is one of the most commonly used indicators of soil health, as it  
22 plays a vital role in maintaining fertility and combating global warming. Understanding  
23 the vertical distribution and controlling factors of organic carbon in the entire regolith,  
24 rather than just the routinely defined upper 1 m portion of the soil, is crucial for  
25 assessing soil health in a holistic perspective. In this study, 21 boreholes in four  
26 different land uses were drilled from the land surface down to the bedrock in a typical  
27 subtropical agricultural watershed. The total organic carbon stock in the regolith ranged  
28 from 77.8 Mg C ha<sup>-1</sup> to 311.8 Mg C ha<sup>-1</sup> and the organic carbon content showed a  
29 progressive decline from land surface to bedrock. However, on average, only 19.0 %  
30 of total organic carbon was stored at the depth 0-30 cm and 17.7% between 30 and 100  
31 cm, whereas 63.3 % was stored below 100 cm. Total organic carbon stock was  
32 significantly higher under paddy fields than under cropland, orchard or woodland in the  
33 upper 100 cm ( $p < 0.05$ ) possibly due to straw incorporation, flooding of the paddy soils  
34 and their position on the lower slopes where eroded soil was deposited. However, there  
35 was no significant difference in total organic carbon stock below 200 cm ( $p > 0.05$ ).  
36 According to the boosted regression tree analysis, soil texture outperformed the other  
37 edaphic factors and was the primary edaphic factor controlling TOC content of the  
38 different soils. The results show that there is a large carbon reservoir in the deep regolith.  
39 Land use strongly affects the distribution of carbon in the top 100 cm soil layers but has  
40 little effect on deep soil organic carbon. Deep TOC were closely linked to soil texture.  
41 This study highlights the importance of deep soil organic carbon for soil health and  
42 understanding the factors controlling its content for improved estimates of soil carbon  
43 storage.

44 **Key words:** deep soil organic carbon; vertical distribution; edaphic factor; land use;

45 Earth's critical zone

## 46 **1. Introduction**

47 Soil is the largest pool of carbon in terrestrial ecosystems and holds twice as much  
48 carbon (C) as the atmosphere (Schlesinger and Bernhardt, 2013). Even a small  
49 percentage change in soil C may introduce significant change in atmospheric CO<sub>2</sub>  
50 concentrations (Lal, 2003). Deep soil organic C (SOC) may comprise a large terrestrial  
51 C pool, but is arguably the least investigated component of the terrestrial C pool (Wade  
52 et al., 2019). Deep SOC is generally unsaturated with low C concentrations (Wang et  
53 al., 2015). Therefore, it has been suggested that more SOC could be sequestered through  
54 enhanced C input into deep soil by root penetration and vertical transport of dissolved  
55 organic C (Lorenz and Lal, 2005), which may have the potential to counterbalance the  
56 current increase in atmospheric CO<sub>2</sub> (Minasny et al., 2017). To this end, the vertical  
57 distribution and stock of deep SOC are important in assessing the potential for soil C  
58 sequestration and for informing related management policies.

59 Deep SOC is mainly sourced from dissolved organic matter, plant roots and root  
60 exudates, bioturbation, and translocation of particulate organic matter and clay-bound  
61 organic matter (Rumpel and Kögel-Knabner, 2011). A key feature of deep SOC is its  
62 slow turnover times at centennial or millennial timescales; the underlying mechanisms  
63 for this slow turnover remain unclear (Jackson et al., 2017; Trumbore, 2009). This  
64 characteristic has been used to support the assumption that deep SOC sequestration is  
65 negligible or resistant to surface environment change (Chabbi et al., 2009; Li et al.,  
66 2021). However, this assumption is likely to overlook the potential of deep soil horizons  
67 in storing high proportions of SOC stocks at depth (Richter and Babbar, 1991).  
68 Moreover, deep SOC may have a significantly different response to global change than  
69 surface soil layers (Bernal et al., 2016). Therefore, quantifying the magnitude and

70 distribution characteristics of deep SOC can provide additional understanding of C  
71 cycling in the whole regolith profile, which will help to improve terrestrial C assessment  
72 and combat global warming.

73 Studies on soil C have historically focussed on shallow soil layers, which limits  
74 our understanding of soil dynamics deep in the soil profile (Harrison et al., 2011). These  
75 studies have explored the stock and distribution of SOC in the topsoil at global  
76 (Arrouays et al., 2014; Hengl et al., 2017), continental (Grunwald et al., 2011; Orgiazzi  
77 et al., 2017), national (Luo et al., 2010), regional (Song et al., 2016) or local scales (Liu  
78 et al., 2016). They have provided a significant contribution to the assessment of the  
79 SOC inventory in the top layers of the soil. However, much less attention has been  
80 given to the stock and spatial distribution of C stored deeper than 20 cm, especially  
81 deeper than 100 cm, which is important for understanding the biogeochemical cycling  
82 of C over longer timescales (Gross and Harrison, 2019; Rumpel and Kögel-Knabner,  
83 2011). It is estimated that these deep SOC reserves are very large. Batjes (1996)  
84 predicted that estimates of global SOC stocks could increase substantially from 1462–  
85 1548 Pg C in the upper 100 cm to 2376–2456 Pg C if the 100 to 200 cm soil layer was  
86 included in the estimates. Jobbágy and Jackson (2000) further reported that global SOC  
87 storage in the top 300 cm of soil was 56% more than that in the top 100 cm (i.e. 2344  
88 Pg C to 300 cm compared to only 1502 Pg C to 100 cm). Other estimates have  
89 emphasized the importance of SOC at different depths or multiple scales (Davidson et  
90 al., 2011; Harper and Tibbett, 2013; Tarnocai et al., 2009). In China's Loess Plateau  
91 with a semi-arid and arid climate, previous studies have showed that deep SOC  
92 contributes significantly to the total soil C budget (Gao et al., 2017; Jia et al., 2020; Li  
93 et al., 2021; Yang et al., 2020a; Yu et al., 2019a). These studies highlighted that an  
94 accurate SOC inventory should include deep soil layers, but data on deep SOC remains

95 scarce, mainly due to the challenges of deep soil sampling, especially in subtropical  
96 humid regions. In these regions, soil organic matter is more rapidly decomposed due to  
97 warmer and wetter environment (Bellè et al., 2022; Don et al., 2011; Yao et al., 2019),  
98 so the deep SOC stock is assumed to be negligible, but with little supporting evidence.  
99 Investigations into the vertical distribution of deep SOC in subtropical regions are,  
100 therefore, urgently needed to fill this knowledge gap.

101 Edaphic properties, such as soil texture and pH, are the innate factors that regulate  
102 SOC stabilization and stocks (Dungait et al., 2012). Physical protection of occluded  
103 particulate SOC is an important stabilisation mechanism (Six et al., 2000), but how this  
104 mechanism functions along the depth gradient is elusive because the processes of  
105 aggregate formation in shallow and deeper soil layers may be quite different (Rumpel  
106 and Kögel-Knabner, 2011). In addition, the variation with depth in soil  
107 physicochemical properties that control the availability of water, nutrients, oxygen and  
108 other resources that are important for the operation of C cycling (Lehmann and Kleber,  
109 2015; Schmidt et al., 2011), needs further investigation. By dividing the regolith (from  
110 land surface to soil-bedrock interface) into shallow (< 100 cm) and deep (> 100 cm)  
111 soil layers, the effects of edaphic properties can be explicitly identified.

112 Unlike the edaphic properties, land use could affect the SOC stock through altered  
113 land cover and management practices (Wang et al., 2015). Although extensive studies  
114 have investigated the impacts of land use (Conforti et al., 2016; Yu et al., 2020b),  
115 knowledge gaps regarding its effect on deep soil layers still exist. Most studies have  
116 focussed only on the upper 100 cm of the soil, which cannot adequately reflect the  
117 impacts of land use on the stock and distribution of SOC in deeper soil layers  
118 (Schwanhart and Jarmer, 2011; Singh et al., 2018). The depth of potential land use  
119 influence on SOC remains poorly defined. By explicitly comparing the stocks of SOC

120 in different land uses at deeper depth, we aim to gain insight into the effect of land use  
121 on the vertical distribution of SOC.

122 Red soils are generally acidic and highly weathered soils, that are widely  
123 distributed in tropical and subtropical regions around the world (Eswaran et al., 2012).  
124 They are approximately equivalent to Acrisols, Alisols and Ferralsols (IUSS Working  
125 Group WRB, 2015) or Ultisols and Oxisols (Soil Survey Staff, 2014). In China, they  
126 cover an area of more than  $2 \times 10^6$  km<sup>2</sup> (Liu et al., 2017) and are the most important  
127 soil resources of southern China. Because of some unfavourable properties (e.g., low  
128 pH and SOC content) and long-term inappropriate management, red soils are often  
129 subject to severe degradation (Wilson et al., 2004). Many studies have suggested that  
130 the quality of degraded red soils could be greatly enhanced by increasing the SOC  
131 content (Gong et al., 2013; Huang et al., 2010; Zhang and Xu, 2005).

132 The SOC content of red soils has been investigated with respect to its spatial  
133 variation (Jiang and Guo, 2019; Zhang et al., 2010), contribution to soil aggregation  
134 (Peng et al., 2015) and to provide estimates of the C pools (Qian et al., 2013). However,  
135 most of these studies have focused only on the upper 100 cm of the soil. As a result,  
136 studies on the spatial distribution and storage of SOC in the deep soil layers are limited,  
137 and the impact of changes in land use on deep SOC also remains poorly understood.  
138 The critical zone approach aims to study the whole regolith, and so provides an  
139 opportunity to investigate C processes in both shallow and deeper soil layers (Yang et  
140 al., 2020c). Determining the vertical distribution and influencing factors of SOC stocks  
141 in a red soil critical zone will allow the potential for C sequestration and maintenance  
142 of the quality and security of soil resources to be more fully assessed (Zhang et al.,  
143 2019).

144 In this study, we assessed the profile distribution of total organic C (TOC) across

145 the entire regolith of a representative subtropical red soil critical zone in a typical  
146 subtropical agricultural watershed. The specific objectives are to (1) evaluate the  
147 vertical distribution of TOC from the land surface to the surface of the bedrock (up to  
148 1950 cm), (2) estimate the TOC storage in the entire regolith, and (3) examine the  
149 effects of edaphic factors and land use on the vertical distribution of TOC.

150

## 151 **2. Materials and methods**

### 152 **2.1 Study area**

153 The study area (116°53'–116°55'N, 28°13'–28°14'E) is near to the well-  
154 established Sunjia Red Soil Critical Zone Observatory (RSCZO), Yingtan, China (Yang  
155 et al., 2020c). It has an area of  $2 \times 2$  km<sup>2</sup> with an altitude that varies from 38 to 74 m  
156 above sea level (Fig. 1), and a mean slope of 2.4°. This area has a subtropical monsoon  
157 climate with a mean annual precipitation of 1795 mm and a mean annual temperature  
158 of 17.8 °C. The land uses were mainly paddy field (area proportion = 28%), cropland  
159 (23%), orchards (9%), woodland (19%), and the other (21%, including ponds, roads,  
160 ditches and buildings). Land management was distinct among the four land uses (Yang  
161 et al., 2020b). The main crops in croplands were peanuts (*Arachis hypogaea*), sweet  
162 potatoes (*Ipomoea batatas*), cassava (*Manihot esculenta*), oilseed rape (*Brassica napus*),  
163 turnips (*Brassica rapa*) and watermelons (*Citrullus lanatus*). The main trees in  
164 woodlands were camphor (*Cinnamomum camphora*) and masson pine (*Pinus*  
165 *massoniana*). Mandarin citrus (*Citrus reticulata* Blanco) and chestnut (*Castanea*  
166 *mollissima* Bl.) were the main orchard trees. The regoliths were developed from the  
167 underlying sandstone and Quaternary red clay as parent materials.

168

169

(Fig.1 is about here)

170

## 171 **2.2 Sample collection and analysis**

172 In March 2018, 21 sampling sites were selected for borehole drilling based on a  
173 careful field investigation (Fig. 1). Among them, 8, 7, 3 and 3 sites were from paddy  
174 field, cropland, orchard and woodland, respectively. The selected sites well represented  
175 the major land management practices, and landscape positions in the catchment (Yang  
176 et al., 2020c). A cylinder with an internal diameter of 13 cm was used to obtain a  
177 continuous core from land surface to fresh bedrock at each site. Soil samples in the  
178 upper 100 cm, 100-500 cm and below 500 cm were collected at 10 cm, 20 cm and 50  
179 cm depth intervals, respectively. For bulk density (BD) measurements, a 100 cm<sup>3</sup>  
180 standard stainless-steel cutting ring was used to collect undisturbed samples from the  
181 centre of each core. Pictures representing the sampling campaign can be seen in Fig. 2.

182

183 **(Fig.2 is about here)**

184 Regolith samples were air-dried, ground in an agate mortar with a pestle and sieved  
185 through a nylon mesh before being used for the analysis of TOC (g kg<sup>-1</sup>), particle-size  
186 distribution (sand, silt and clay content; % by volume) and pH (H<sub>2</sub>O). BD is a weighted  
187 average of the densities of its material components in which TOC is an important part.  
188 pH indicates the soil acid-base environment which is vital for microbe to process SOC.  
189 Water content (WC) is related to hydrological processes which determine the erosion  
190 and deposition of particles. Particle-size distribution may impact the accumulation of  
191 SOC in minerals (Six et al., 2002). For the above reasons, we selected them as potential  
192 influencing factors for analysis in the present study.

193 TOC was measured by the K<sub>2</sub>Cr<sub>2</sub>O<sub>7</sub>-H<sub>2</sub>SO<sub>4</sub> wet oxidation method of the Walkley-  
194 Black procedure (Nelson and Sommers, 1982). Particle-size distribution was measured



195 using a Beckman Coulter LS230 laser diffraction particle size analyser (Zhang and  
196 Gong, 2012). pH was measured using a digital pH meter in a 1:2.5 soil: water solution.  
197 BD ( $\text{g cm}^{-3}$ ) was measured by drying the sample to a constant weight at 105 °C. WC  
198 was determined by drying the field-moist samples at 105 °C to a constant weight for  
199 about 12 hours. Descriptive statistics of the above properties are presented in Figs. S1-  
200 3. Further physicochemical properties for each individual borehole can be found in  
201 previous studies (Yang et al., 2020b, c).

202 Cumulative TOC stock was calculated using the following equation (Jia et al.,  
203 2020):

$$204 \quad S_h = \sum_{i=1}^n \frac{BD_i \times TOC_i \times T_i \times (1 - \theta_i)}{10} \quad (1)$$

205 where  $S_h$  represents the cumulative TOC stock ( $\text{Mg C ha}^{-1}$ ) within a certain depth  
206 interval  $h$  (cm) which consist of  $n$  layers in total;  $BD_i$ ,  $TOC_i$  and  $T_i$  are respectively the  
207 BD ( $\text{g cm}^{-3}$ ), TOC ( $\text{g kg}^{-1}$ ) and thickness (cm) of the  $i^{\text{th}}$  layer; and  $\theta_i$  is the volume  
208 percentage of gravel ( $> 2$  mm) of the  $i$ th layer (%). As described above, samples were  
209 collected at 10, 20 and 50 cm depth intervals and the regolith thickness varied among  
210 boreholes, so  $T_i$  is 10, 20 and 50 cm at depth 0-100 cm, 100-500 cm and below 500 cm,  
211 respectively.

212

### 213 **2.3 Statistical analysis**

214 Pearson correlation analysis was used to determine the relationship between TOC  
215 and regolith physicochemical properties. A one-way analysis of variance followed by a  
216 least significant difference test ( $p < 0.05$ ) was conducted by using the *agricolae* package  
217 (Mendiburu, 2019). The *ggplot2* package (Wickham, 2016) was used to produce  
218 statistical plots.

219 In order to quantify the relative importance of regolith properties in explaining the

220 vertical variability of TOC, we applied the boosted regression tree (BRT) model using  
221 data from depths 0-100 cm and 100 cm - bedrock respectively. BRT is a commonly  
222 used machine learning algorithm developed by Friedman et al. (2000), which combines  
223 two powerful statistical algorithms: boosting and regression trees. The boosting  
224 algorithm develops a final model by iterating and progressively adding trees to the  
225 model. Regression trees were used to analyze the relationship between response  
226 variable and explanatory variables, in which a binary split was applied to fit a simple  
227 model to each resulting section (Wang et al., 2017). Compared with other machine  
228 learning algorithms, BRT model has been evidenced to have a high predictive accuracy  
229 and good interpretability of the relationship between variables (Müller et al., 2013). The  
230 BRT model was conducted with the *dismo* (Hijmans et al., 2017) and *gbm* (Elith et al.,  
231 2008) packages.

232 All the above analyses were conducted with R language (R Core Team, 2021).

233

### 234 **3. Results**

#### 235 **3.1 Vertical distribution of total organic carbon**

236 Vertical patterns of TOC contents from the land surface to the soil-bedrock  
237 interface for the boreholes are shown in Fig. 3. The TOC contents decreased with  
238 increasing depth, especially rapidly in the first 50 cm soil layer. Below that depth, TOC  
239 showed a slower decline. The highest TOC content ( $29.6 \text{ g kg}^{-1}$ ) was observed at depth  
240 0–10 cm of paddy field regolith (P1), whereas the lowest TOC ( $3.8 \text{ g kg}^{-1}$ ) at the same  
241 depth was observed in the orchard (O3). The mean TOC at depth 0–10 cm was  $12.5 \text{ g}$   
242  $\text{kg}^{-1}$ . Generally, the TOC contents in deep soils were almost constant and at a low level,  
243 and our results showed that the mean TOC content below 100 cm was only  $1.2 \text{ g kg}^{-1}$ ,  
244 while the corresponding values for the first 30 cm and 100 cm were  $7.5 \text{ g kg}^{-1}$  and  $4.1$

245 g kg<sup>-1</sup>, respectively.

246

247

(**Fig.3** is about here)

248

249 The means and standard deviations of TOC stocks at different depth intervals (0-  
250 30 cm, 30-100 cm, 0-100 cm, and 100 cm - bedrock) are shown in Table 1. The  
251 cumulative TOC stocks at depth 0-30 cm were  $44.2 \pm 9.0$  Mg C ha<sup>-1</sup>,  $21.4 \pm 4.2$  Mg C  
252 ha<sup>-1</sup>,  $23.9 \pm 7.1$  Mg C ha<sup>-1</sup> and  $17.9 \pm 5.1$  Mg C ha<sup>-1</sup> for paddy field, cropland, woodland  
253 and orchard, respectively. The cumulative TOC stocks at depth 0-100 cm were  
254 significantly higher in paddy fields than in other land uses;  $79.5 \pm 16.0$  Mg C ha<sup>-1</sup> for  
255 paddy fields,  $47.3 \pm 6.6$  Mg C ha<sup>-1</sup> for orchards,  $45.4 \pm 9.2$  Mg C ha<sup>-1</sup> for woodland and  
256  $41.2 \pm 5.3$  Mg C ha<sup>-1</sup> for cropland.

257

258

(**Table 1** is about here)

259

260 The cumulative distribution and proportion of TOC stock for the boreholes are  
261 shown in Fig. 4. The cumulative TOC stock throughout the regolith ranged from 77.8  
262 Mg C ha<sup>-1</sup> in cropland regolith 1 (C1) to 311.8 Mg C ha<sup>-1</sup> in paddy field regolith 7 (P7).  
263 The ratio of TOC stored below 100 cm to the TOC in the top 100 cm ranged from 0.7  
264 in paddy field regolith 4 (P4) to 6.7 in woodland regolith 3 (W3). The percentage of  
265 TOC in the whole regolith that was stored at depth 0-30 cm ranged from 7.1% in orchard  
266 regolith 3 (O3) to 30.9 % in paddy regolith 8 (P8), with a mean of 19.0 %. On average,  
267 only 36.7 % of TOC was stored in the upper 100 cm, of which 19.0% was stored within  
268 depth 0-30 cm (tillage layer). Detailed information on the cumulative TOC stock for  
269 each individual depth increment can be found in Fig. S4.

270

271

(Fig.4 is about here)

272

### 273 **3.2 Relative importance of edaphic factors**

274 Fig. 5 shows the Pearson correlation between TOC and selected edaphic factors  
275 for the depths of 0-100 cm and 100 cm-bedrock, respectively. Fig. 6 shows the results  
276 of BRT analysis on data at depths 0-100 cm and 100 cm-bedrock, respectively. For the  
277 0-100 cm section, WC was identified as an important influencing factor (relative  
278 importance = 34.15%), followed by BD (24.05%), sand (14.59%), clay (12.14%), silt  
279 (7.71%) and pH (7.37%). Soil texture (represented by sand, clay and silt) explained  
280 34.44% of the variability in total, and was determined as the most important influencing  
281 factor for this section. For the 100 cm-bedrock section, pH was an important factor  
282 (25.27%), followed by BD (23.67%), clay (22.12%), sand (12.45%), WC (9.07%) and  
283 silt (7.43%). Similar to the 0-100 cm section, soil texture has a relatively high  
284 importance (42%). Overall, soil texture was the primary controlling factor for both 0-  
285 100 cm (34.44%) and 100 cm-bedrock (42%).

286

287

(Fig.5 is about here)

288

(Fig.6 is about here)

289

### 290 **3.3 Total organic carbon at different regolith depths among different land use** 291 **types**

292 The vertical distribution of TOC in paddy field, cropland, orchard and woodland  
293 are shown in Fig. 7. In general, they all showed a depletion pattern with increasing  
294 depth from land surface to 500 cm. The TOC content for each land use was significantly

295 greater in the upper layers (0-20 cm) than that in the lower layers (> 20 cm). However,  
296 differences both between land uses and with depth can still be identified. The TOC  
297 content range across the entire profile was 0.9-21.4 g kg<sup>-1</sup> for paddy fields, 1.0-7.3 g  
298 kg<sup>-1</sup> for cropland, 1.0-5.8 g kg<sup>-1</sup> for orchards and 0.7-7.7 g kg<sup>-1</sup> for woodland.  
299 Significant differences among the four land uses were observed only in the upper 90  
300 cm. The paddy fields had higher TOC contents than the other land uses in almost all  
301 layers in the upper 90 cm. By contrast, cropland had the lowest TOC contents in almost  
302 all layers.

303

304 (Fig.7 is about here)

305

306 We compared the statistically significant difference in TOC stock among land uses  
307 at different depths (Fig. 8). The TOC stock was significantly higher under paddy field  
308 than under other land uses at depths 0-30 and 0-100 cm. Below depth 100 cm, there  
309 was no significant difference in TOC stock among the four land uses despite the TOC  
310 stock under paddy field having a higher variation. In the vertical direction, a similar  
311 pattern was observed among the different land uses with peak stock at depth 0-100 cm.  
312 Under cropland, orchard and woodland, there was no significant difference in TOC  
313 stock at depths 0-30 cm, 100-200 cm or 200-300 cm. However, this was not the case in  
314 the paddy fields. For paddy fields, the TOC stored at 0-30 cm was significantly greater  
315 than that stored at 200-300 cm.

316

317 (Fig.8 is about here)

318

319 **4. Discussion**

#### 320 **4.1 Importance of deep total organic carbon pool in the critical zone**

321 Our results showed that the mean TOC concentration within the top 100 cm of the  
322 soil was 3.4 times greater than the concentration below 100 cm (Fig. 3; 4.1 vs. 1.2 g kg<sup>-1</sup>).  
323 The lower concentration of TOC below 100 cm is as expected, due to the lower  
324 biomass inputs (Hu et al., 2014). However, because of the large depth of the regolith,  
325 which was observed to have a mean depth of 770 cm (Yang et al., 2020b), the TOC  
326 stock below 100 cm was 2.1 times greater than that stored in the top 100 cm (Fig. S4).  
327 On average, 63.3 % of TOC was stored below 100 cm (Fig. 4). Jia et al. (2020) also  
328 reported that the storage of SOC mainly depended on soil depth. This finding strongly  
329 supports our hypothesis that the largest proportion of the TOC is stored below 100 cm.  
330 It is also in agreement with the assertion of previous studies (Borchard et al., 2019;  
331 Harper and Tibbett, 2013; Hobbey and Wilson, 2016; Jobbágy and Jackson, 2000; Wade  
332 et al., 2019) that TOC in deep layers should not be ignored when estimating the  
333 inventory of TOC in terrestrial ecosystems. Therefore, TOC stored in deep regoliths  
334 should be taken into account to avoid the systematic underestimation of TOC stocks.  
335 Moreover, these deep TOC stocks may respond differently to the global warming  
336 compared with TOC in the surface soils (Harper and Tibbett, 2013; Harrison et al., 2011;  
337 Rumpel and Kögel-Knabner, 2011). This finding may also be applied to the other  
338 tropical and subtropical regions around the world that have similarly thick regoliths. To  
339 date, no study has estimated TOC in the entire critical zone at a global, continental or  
340 even national level, so we do not know the true size of the terrestrial C pool. Future  
341 critical zone studies should attempt to fill this knowledge gap.

342

#### 343 **4.2 Effect of edaphic factors on total organic carbon storage**

344 Past studies have evidenced that edaphic factors govern the stability and

345 decomposition of TOC (Hemingway et al., 2019; Lehmann and Kleber, 2015; Schmidt  
346 et al., 2011; Xu et al., 2016), and thereby affect the vertical distribution of TOC (Cao  
347 et al., 2021). Our results showed that soil texture was the most important edaphic factor  
348 affecting TOC variation in the whole regolith (Fig. 6). For the 0-100 cm section, sand  
349 (14.59%), clay (12.14%) and silt (7.71%) jointly explained 34.44% of the variability in  
350 TOC; for the 100 cm – bedrock section, clay (22.12%), silt (12.45%) and sand (7.43%)  
351 combined accounted for 42% of the relative importance (Fig. 6). Of the three texture  
352 variables, clay content showed the greatest effect on TOC. This is likely to be due to  
353 significant impacts of soil clay on the formation and transformation of soil aggregates  
354 which regulate access of micro-organisms and nutrients to the TOC (Luo et al., 2021;  
355 Sun et al., 2020). Decomposition of TOC can be reduced if it is occluded within soil  
356 aggregates and/or adsorbed onto mineral surfaces (Six et al., 2000). Previous studies  
357 have found that clay minerals play an important role in stabilizing subsoil TOC (Dick  
358 et al., 2005; Rumpel and Kögel-Knabner, 2011; Six et al., 2002; Wade et al., 2019).  
359 Soil clay can greatly increase C accumulation and stabilization due to its effect on  
360 mineral surface area and the formation of soil aggregates (Fernandez et al., 2019).  
361 Therefore, the capacity for TOC sequestration is enhanced as the soil clay content  
362 increases (Mathieu et al., 2015).

363 Soil WC contributed greatly to the variation in TOC (Yu et al., 2019a). Our study  
364 showed that WC has a significant effect on the TOC stocks at depths of 0-100 cm (Fig.  
365 6). The WC explained 34.15% and 9.07% of the variability in TOC concentration for  
366 the 0-100 cm section and the 100 cm-bedrock section, respectively. This is consistent  
367 with other reports that WC can affect the decomposition, mineralization and  
368 transformation of TOC (Davidson et al., 2000; Yu et al., 2019a). While losses of TOC  
369 by decomposition increase with WC up to field capacity in the shallow soils, but plant

370 growth also increases the C inputs to the soil (Mayer et al., 2019; Yang et al., 2020a).  
371 Therefore, with sufficient water-availability, organic matter can accumulate and be  
372 transported down into the soil profile. By contrast, WC in deep soils tends to stay at a  
373 relatively stable level (Fig. S2), so its effect on TOC accumulation in deep soils  
374 decreases with increasing depth compared to that in the shallow soil.

375 In this study, BD had an important influence on TOC stocks (Fig. 6). Soil BD is  
376 the weighted average of the densities of its components including soil minerals, TOC,  
377 and air- or water-filled pores (Yang et al., 2014). It is closely related to soil porosity,  
378 water infiltration and solute transport in the whole soil profile (Kojima et al., 2018; Lu  
379 et al., 2019). Soil porosity has been found to strongly influence dissolved organic C  
380 leaching in both surface and subsurface soils (Liu et al., 2019; McGlynn and McDonnell,  
381 2003; Niu et al., 2021; Rizinjirabake et al., 2019). Soil BD can also impact the oxygen  
382 available for microbial decomposition of organic matter (Six et al., 2002). In our study,  
383 BD increased from 1.3 to 1.5 g cm<sup>-3</sup> from 0-10 cm to 180-200 cm (Fig. S2), which may  
384 affect the transport of dissolved organic C (Kojima et al., 2018). Furthermore, because  
385 of the increase of soil BD and therefore the decrease of soil porosity with increasing  
386 depth, the transport of dissolved oxygen will be inhibited, so that the microbial  
387 decomposition of organic matter will be limited. Thus, BD strongly influences the  
388 variation in TOC throughout the whole soil profile.

389 The results showed that pH strongly influenced TOC (Fig. 5 and 6). This is  
390 supported by past studies that have suggested that soil pH can mediate the  
391 decomposition of TOC (Hagedorn et al., 2012; Tonon et al., 2010). Decomposition of  
392 soil organic matter is mainly conducted by microbial processes, so changes in the  
393 microbial community and enzymes produced influence the decomposition rate (Zhang  
394 et al., 2020). Our previous studies have shown that substantial bacterial communities



395 relating to acidification exist even at the bottom of a 6.2 m red soil profile (Wu et al.,  
396 2019b; Zhao et al., 2019). It has been reported that a lower pH will significantly depress  
397 microbial activities during soil organic matter decomposition and therefore decrease  
398 microbial-derived C accumulation but also result in slower decomposition and so  
399 increased TOC (Kemmitt et al., 2006; Liu et al., 2014). Low soil pH can also facilitate  
400 the chemical and physical protection of TOC. The decrease in soil pH can increase the  
401 positive charges of variable charge minerals, which has been observed to increase  
402 organic matter adsorption (McBride, 1994; Spielvogel et al., 2008). The decrease in soil  
403 pH would also depress the ionization of organic acids, so weakening the repulsion  
404 between negatively-charged clays and organic matter in aggregates (Sparks, 2003;  
405 Zhang et al., 2020). This explains the observed importance of soil pH in controlling the  
406 variation in TOC.

407

#### 408 **4.3 Effect of land use on total organic carbon storage**

409 The TOC in the four land-use types considered all showed similar exponential  
410 patterns of decline down the soil profile (Fig. 7). Land use only markedly impacted  
411 TOC to a depth of 200 cm, with significant differences between the four land-use types  
412 only being observed in the upper 100 cm (Fig. 7). Below 200 cm, no significant effect  
413 of land use was observed in the TOC stocks (Fig. 8). This is in contrast to observations  
414 in the Loess Plateau, where a number of authors have reported significant differences  
415 at depths below 200 cm (Jia et al., 2017; Wang et al., 2016; Yu et al., 2019b). This  
416 could be due to buried soil layers in the Loess Plateau, which may contain a large  
417 amount of C (Jia et al., 2020), but could also be due to the dry climate under which deep  
418 rooting systems develop and fine roots increase the TOC in the deep soil layers (Niu et  
419 al., 2021). Some of the woodlands included in this study were only converted from the

420 other land uses in the year 2000 (Yang et al., 2020b), so any changes in TOC due to  
421 land use would not have had sufficient time to move down the regolith.

422 The mean TOC stocks in the top 100 cm under the paddy fields ( $79.5 \text{ Mg C ha}^{-1}$ )  
423 were significantly higher than those under the other three land uses ( $47.3 \text{ Mg C ha}^{-1}$  for  
424 orchard,  $45.4 \text{ Mg C ha}^{-1}$  for woodland and  $41.2 \text{ Mg C ha}^{-1}$  for cropland) (Fig. 8).  
425 Woodland is considered to have a large C input from above ground biomass (Lal, 2004),  
426 but its effect in this study was not significant. The greater TOC stocks in the paddy  
427 fields relative to other land uses can partially be explained by higher TOC inputs due  
428 to the straw being ploughed into the soil rather than being burned or removed (Li et al.,  
429 2010; Zhu et al., 2010). This is now a typical practice for most paddy fields in China.  
430 In a study conducted at national scale, Zhao et al. (2018) reported the average SOC  
431 stock in the topsoil of cropland had increased from  $28.6 \text{ Mg C ha}^{-1}$  in 1980 to  $32.9 \text{ Mg}$   
432  $\text{C ha}^{-1}$  in 2011, and this was largely attributed to crop residue inputs. In our study area,  
433 it is common practice to incorporate straw in paddy fields, while no similar practice is  
434 used in the other land uses. The long-term cultivation history of paddy fields may also  
435 strengthen the impact of repeated inputs of straw to the soil. Wu et al. (2019a) reported  
436 that the old paddy fields in our study area had been cultivated for over 100 years, so  
437 would be expected to be in steady state with respect to the inputs, while the main tree  
438 species in the woodland were just older than 30 years.

439 The second reason for the high C content in the top 100 cm in the paddy fields  
440 may be due to the slower decomposition rate of SOC due to the saturated condition of  
441 the soil (Li et al., 2010; Zhang and He, 2004). Unlike the other land uses, paddy fields  
442 are flooded with an approximately 5 cm deep layer of water for most of the growing  
443 season, which creates a water saturation zone. Mayer et al. (2019) reported that water  
444 saturation in agricultural soil slows decomposition of SOC, resulting in high subsoil

445 (30–100 cm) SOC content.

446        However, perhaps the most important reason for the higher TOC content in the top  
447 100 cm of the paddy fields could be their landscape location, which is usually on the  
448 lower slopes, where soil is likely to be deposited following erosion from the upper  
449 slopes (Boix-Fayos et al., 2009). Therefore, paddy fields are likely to accumulate  
450 nutrients and fine soil particles, resulting in an inherently higher TOC content of the  
451 paddy soils due to topography (Singh et al., 2018).

452

#### 453 **4.4 Limitations and future studies**

454        By expanding from subsurface 0-100 cm soil layers to the profile of the entire  
455 regolith, this study has provided an important investigation into the vertical distribution  
456 of TOC in a typical red soil critical zone. However, there remain some limitations  
457 associated with the study design that should be noted.

458        The study cannot directly compare the relative importance of land use and edaphic  
459 factors on the TOC distribution. This is because land use was not included in the BRT  
460 analysis alongside the edaphic factors. Land use is a categorical variable while edaphic  
461 factors can be treated as numerical. Although the BRT model can deal with categorical  
462 and numerical variables at the same time, this complicates explanation of the model  
463 results, so was not done. The study also did not account for any potential changes in  
464 edaphic factors over time. This is a reasonable assumption for stable characteristics,  
465 such as soil texture, but may introduce uncertainty for factors, such as soil moisture,  
466 which are highly dynamic. However, the moisture content of deep soil layers is more  
467 stable, so this is not likely to be a problem at depth (Yang et al., 2012). Because the  
468 study did not account for the impact of topography on the TOC content, this may have  
469 affected the findings with respect to some land uses, such as paddy soils. Topographic

470 factors distribute organic matter down a slope by erosion-deposition processes (Yu et  
471 al., 2020a). Future studies could provide explicit assessment of the impact of  
472 topographical features of TOC distribution.

473 All 21 boreholes showed a similar exponential-depletion pattern of TOC content  
474 down the profile, independent of land use, while significant differences existed in TOC  
475 stock between different land uses in the top 100 cm soil layers. This suggests that land  
476 use had little impact on the TOC in the deeper part of the regolith. Therefore, it may be  
477 possible to provide regional estimates of deep TOC stocks simply by fitting a depth  
478 function (Bishop et al., 1999; Liu et al., 2016). Based on this assumption, Song et al.  
479 (2019) mapped the three-dimensional distribution of deep organic matter in the RSCZO.  
480 However, the degree of decline in the upper soil layers varied among different land uses;  
481 paddy fields showed a more rapid decrease in TOC than other land uses, so the effect  
482 of land use should be taken into account when developing depth functions to estimate  
483 TOC stocks (Liu et al., 2016). Furthermore, the time since land use change can have a  
484 significant effect on the distribution and amount of TOC deep in the regolith (Zhou et  
485 al., 2019), so further research is needed to explicitly investigate the impact of time since  
486 land use change on TOC deep in the regolith profile.

487

## 488 **5. Conclusions**

489 The TOC content and stock generally showed exponential depletion patterns from  
490 the land surface to the surface of the bedrock. On average, 63.3 % of TOC was stored  
491 below 100 cm, which confirmed the importance of deep soil when estimating SOC  
492 inventory in tropical and subtropical regions. Land use significantly affect the vertical  
493 distribution of TOC in the upper 100 cm, but did not markedly affect it below 200 cm.  
494 Soil texture was identified as the primary edaphic factor controlling TOC content of the

495 different soils. This study provides important evidence to better understand deep soil C  
496 cycling and to provide better estimates of terrestrial C storage.

497

#### 498 **Acknowledgement**

499 This study was financially supported by the National Key Research and  
500 Development Plan of China (2018YFE0107000), the National Natural Science  
501 Foundation of China (42107334), the Second Tibetan Plateau Scientific Expedition and  
502 Research Program (2019QZKK0306), and the China Postdoctoral Science Foundation  
503 (2021TQ0337, 2021M703305). Special thanks go to our colleagues of Soils in Time  
504 and Space team for their help during field survey and laboratory analysis.

505

#### 506 **Appendix A. Supplementary data**

507 The following are the Supplementary data to this article:

508 Supplementary data 1.

509

#### 510 **References**

- 511 Arrouays, D., Grundy, M.G., Hartemink, A.E., Hempel, J.W., Heuvelink, G.B.M.,  
512 Hong, S.Y., Lagacherie, P., Lelyk, G., McBratney, A.B., McKenzie, N.J.,  
513 Mendonca-Santos, M.d.L., Minasny, B., Montanarella, L., Odeh, I.O.A.,  
514 Sanchez, P.A., Thompson, J.A. and Zhang, G.-L., 2014. Chapter Three -  
515 GlobalSoilMap: Toward a Fine-Resolution Global Grid of Soil Properties. In:  
516 L.S. Donald (Editor), *Advances in Agronomy*. Academic Press, 125: 93-134.
- 517 Batjes, N.H., 1996. Total carbon and nitrogen in the soils of the world. *European*  
518 *Journal of Soil Science*, 47(2): 151-163.
- 519 Bellè, S.-L., Riotte, J., Sekhar, M., Ruiz, L., Schiedung, M. and Abiven, S., 2022. Soil  
520 organic carbon stocks and quality in small-scale tropical, sub-humid and semi-  
521 arid watersheds under shrubland and dry deciduous forest in southwestern India.  
522 *Geoderma*, 409: 115606.
- 523 Bernal, B., McKinley, D.C., Hungate, B.A., White, P.M., Mozdzer, T.J. and Megonigal,  
524 J.P., 2016. Limits to soil carbon stability; Deep, ancient soil carbon  
525 decomposition stimulated by new labile organic inputs. *Soil Biology &*  
526 *Biochemistry*, 98: 85-94.
- 527 Bishop, T.F.A., McBratney, A.B. and Laslett, G.M., 1999. Modelling soil attribute  
528 depth functions with equal-area quadratic smoothing splines. *Geoderma*, 91(1):

- 529 27-45.
- 530 Boix-Fayos, C., de Vente, J., Albaladejo, J. and Martínez-Mena, M., 2009. Soil carbon  
531 erosion and stock as affected by land use changes at the catchment scale in  
532 Mediterranean ecosystems. *Agriculture, Ecosystems & Environment*, 133(1):  
533 75-85.
- 534 Borchard, N., Bulusu, M., Meyer, N., Rodionov, A., Herawati, H., Blagodatsky, S.,  
535 Cadisch, G., Welp, G., Amelung, W. and Martius, C., 2019. Deep soil carbon  
536 storage in tree-dominated land use systems in tropical lowlands of Kalimantan.  
537 *Geoderma*, 354: 113864.
- 538 Cao, Q., Li, J., Wang, G., Wang, D., Xin, Z., Xiao, H. and Zhang, K., 2021. On the  
539 spatial variability and influencing factors of soil organic carbon and total  
540 nitrogen stocks in a desert oasis ecotone of northwestern China. *CATENA*, 206:  
541 105533.
- 542 Chabbi, A., Kögel-Knabner, I. and Rumpel, C., 2009. Stabilised carbon in subsoil  
543 horizons is located in spatially distinct parts of the soil profile. *Soil Biology &  
544 Biochemistry*, 41(2): 256-261.
- 545 Conforti, M., Lucà, F., Scarciglia, F., Matteucci, G. and Buttafuoco, G., 2016. Soil  
546 carbon stock in relation to soil properties and landscape position in a forest  
547 ecosystem of southern Italy (Calabria region). *CATENA*, 144: 23-33.
- 548 Davidson, E., Lefebvre, P.A., Brando, P.M., Ray, D.M., Trumbore, S.E., Solorzano,  
549 L.A., Ferreira, J.N., Bustamante, M.M.d.C. and Nepstad, D.C., 2011. Carbon  
550 inputs and water uptake in deep soils of an Eastern Amazon forest. *Forest  
551 Science*, 57(1): 51-58.
- 552 Davidson, E.A., Trumbore, S.E. and Amundson, R., 2000. Soil warming and organic  
553 carbon content. *Nature*, 408(6814): 789-790.
- 554 Dick, D.P., Nunes Gonçalves, C., Dalmolin, R.S.D., Knicker, H., Klamt, E., Kögel-  
555 Knabner, I., Simões, M.L. and Martin-Neto, L., 2005. Characteristics of soil  
556 organic matter of different Brazilian Ferralsols under native vegetation as a  
557 function of soil depth. *Geoderma*, 124(3): 319-333.
- 558 Don, A., Schumacher, J. and Freibauer, A., 2011. Impact of tropical land-use change  
559 on soil organic carbon stocks—a meta-analysis. *Global Change Biology*, 17(4):  
560 1658-1670.
- 561 Dungait, J.A.J., Hopkins, D.W., Gregory, A.S. and Whitmore, A.P., 2012. Soil organic  
562 matter turnover is governed by accessibility not recalcitrance. *Global Change  
563 Biology*, 18(6): 1781-1796.
- 564 Elith, J., Leathwick, J.R. and Hastie, T., 2008. A working guide to boosted regression  
565 trees. *Journal of Animal Ecology*, 77(4): 802-813.
- 566 Eswaran, H., Reich, P.F. and Padmanabhan, E., 2012. World soil resources:  
567 Opportunities and challenges. In: R.L.e.a. (Eds.) (Editor), *World Soil Resources  
568 and Food Security*. CRC Press, Boca Raton, pp. 29-51.
- 569 Fernandez, R., Frasier, I., Quiroga, A. and Noellemeyer, E., 2019. Pore morphology  
570 reveals interaction of biological and physical processes for structure formation  
571 in soils of the semiarid Argentinean Pampa. *Soil & Tillage Research*, 191: 256-  
572 265.
- 573 Friedman, J., Hastie, T. and Tibshirani, R., 2000. Additive logistic regression: A  
574 statistical view of boosting. *Annals of Statistics*, 28(2): 337-407.
- 575 Gao, X., Meng, T. and Zhao, X., 2017. Variations of Soil Organic Carbon Following  
576 Land Use Change on Deep-Loess Hillslopes in China. *Land Degradation &  
577 Development*, 28(7): 1902-1912.
- 578 Gong, X., Liu, Y.Q., Li, Q.L., Wei, X.H., Guo, X.M., Niu, D.K., Zhang, W.Y., Zhang,

579 J.X. and Zhang, L., 2013. Sub-tropic degraded red soil restoration: Is soil  
580 organic carbon build-up limited by nutrients supply. *Forest Ecology and*  
581 *Management*, 300: 77-87.

582 Gross, C.D. and Harrison, R.B., 2019. The case for digging deeper: Soil organic carbon  
583 storage, dynamics, and controls in our changing world. *Soil Systems*, 3(2): 28.

584 Grunwald, S., Thompson, J. and Boettinger, J., 2011. Digital soil mapping and  
585 modeling at continental scales: Finding solutions for global issues. *Soil Science*  
586 *Society of America Journal*, 75(4): 1201-1213.

587 Hagedorn, F., Kammer, A., Schmidt, M.W.I. and Goodale, C.L., 2012. Nitrogen  
588 addition alters mineralization dynamics of <sup>13</sup>C-depleted leaf and twig litter and  
589 reduces leaching of older DOC from mineral soil. *Global Change Biology*, 18(4):  
590 1412-1427.

591 Harper, R.J. and Tibbett, M., 2013. The hidden organic carbon in deep mineral soils.  
592 *Plant & Soil*, 368(1): 641-648.

593 Harrison, R.B., Footen, P.W. and Strahm, B.D., 2011. Deep Soil Horizons:  
594 Contribution and Importance to Soil Carbon Pools and in Assessing Whole-  
595 Ecosystem Response to Management and Global Change. *Forest Science*, 57(1):  
596 67-76.

597 Hemingway, J.D., Rothman, D.H., Grant, K.E., Rosengard, S.Z., Eglinton, T.I., Derry,  
598 L.A. and Galy, V.V., 2019. Mineral protection regulates long-term global  
599 preservation of natural organic carbon. *Nature*, 570(7760): 228-231.

600 Hengl, T., Mendes de Jesus, J., Heuvelink, G.B.M., Ruiperez Gonzalez, M., Kilibarda,  
601 M., Blagotić, A., Shangguan, W., Wright, M.N., Geng, X., Bauer-  
602 Marschallinger, B., Guevara, M.A., Vargas, R., MacMillan, R.A., Batjes, N.H.,  
603 Leenaars, J.G.B., Ribeiro, E., Wheeler, I., Mantel, S. and Kempen, B., 2017.  
604 SoilGrids250m: Global gridded soil information based on machine learning.  
605 *PLoS ONE*, 12(2): e0169748.

606 Hijmans, R.J., Phillips, S., Leathwick, J. and Elith, J., 2017. dismo: Species Distribution  
607 Modeling. R Package Version 1.1-4.

608 Hobley, E.U. and Wilson, B., 2016. The depth distribution of organic carbon in the soils  
609 of eastern Australia. *Ecosphere*, 7(1): e01214.

610 Hu, X.F., Du, Y., Guan, C.L., Xue, Y. and Zhang, G.L., 2014. Color variations of the  
611 Quaternary Red Clay in southern China and its paleoclimatic implications.  
612 *Sedimentary Geology*, 303: 15-25.

613 Huang, S., Peng, X., Huang, Q. and Zhang, W., 2010. Soil aggregation and organic  
614 carbon fractions affected by long-term fertilization in a red soil of subtropical  
615 China. *Geoderma*, 154(3): 364-369.

616 IUSS Working Group WRB, 2015. World reference base for soil resources 2014,  
617 Update 2015, International soil classification system for naming soils and  
618 creating legends for soil maps. International soil classification system for  
619 naming soils and creating legends for soil maps. Food and Agriculture  
620 Organization of the United Nations, Rome, Italy.

621 Jackson, R.B., Lajtha, K., Crow, S.E., Hugelius, G., Kramer, M.G. and Piñeiro, G.,  
622 2017. The Ecology of Soil Carbon: Pools, Vulnerabilities, and Biotic and  
623 Abiotic Controls. *Annual Review of Ecology, Evolution, and Systematics*, 48(1):  
624 419-445.

625 Jia, X., Wu, H., Shao, M.a., Huang, L., Wei, X., Wang, Y. and Zhu, Y., 2020. Re-  
626 evaluation of organic carbon pool from land surface down to bedrock on China's  
627 Loess Plateau. *Agriculture, Ecosystems & Environment*, 293: 106842.

628 Jia, X.-X., Yang, Y., Zhang, C.-C., Shao, M.-A. and Huang, L.-M., 2017. A State-Space

629 analysis of soil organic carbon in China's Loess Plateau. *Land Degradation &*  
630 *Development*, 28(3): 983-993.

631 Jiang, Y.F. and Guo, X., 2019. Stoichiometric patterns of soil carbon, nitrogen, and  
632 phosphorus in farmland of the Poyang Lake region in Southern China. *Journal*  
633 *of Soils and Sediments*, 19(10): 3476-3488.

634 Jobbágy, E.G. and Jackson, R.B., 2000. The vertical distribution of soil organic carbon  
635 and its relation to climate and vegetation. *Ecological Applications*, 10(2): 423-  
636 436.

637 Kemmitt, S.J., Wright, D., Goulding, K.W.T. and Jones, D.L., 2006. pH regulation of  
638 carbon and nitrogen dynamics in two agricultural soils. *Soil Biology &*  
639 *Biochemistry*, 38(5): 898-911.

640 Kojima, Y., Heitman, J.L., Sakai, M., Kato, C. and Horton, R., 2018. Bulk density  
641 effects on soil hydrologic and thermal characteristics: A numerical investigation.  
642 *Hydrological Processes*, 32(14): 2203-2216.

643 Lal, R., 2003. Global potential of soil carbon sequestration to mitigate the greenhouse  
644 effect. *Critical Reviews in Plant Sciences*, 22(2): 151-184.

645 Lal, R., 2004. Soil carbon sequestration impacts on global climate change and food  
646 security. *Science*, 304(5677): 1623-1627.

647 Lehmann, J. and Kleber, M., 2015. The contentious nature of soil organic matter. *Nature*,  
648 528(7580): 60-68.

649 Li, B.-B., Li, P.-P., Yang, X.-M., Xiao, H.-B., Xu, M.-X. and Liu, G.-B., 2021. Land-  
650 use conversion changes deep soil organic carbon stock in the Chinese Loess  
651 Plateau. *Land Degradation & Development*, 32(1): 505-517.

652 Li, Z.P., Han, C.W. and Han, F.X., 2010. Organic C and N mineralization as affected  
653 by dissolved organic matter in paddy soils of subtropical China. *Geoderma*,  
654 157(3): 206-213.

655 Liu, F., Rossiter, D.G., Song, X.D., Zhang, G.L., Yang, R.M., Zhao, Y.G., Li, D.C. and  
656 Ju, B., 2016. A similarity-based method for three-dimensional prediction of soil  
657 organic matter concentration. *Geoderma*, 263: 254-263.

658 Liu, H., Zak, D., Rezanezhad, F. and Lennartz, B., 2019. Soil degradation determines  
659 release of nitrous oxide and dissolved organic carbon from peatlands.  
660 *Environmental Research Letters*, 14(9): 094009.

661 Liu, W., Jiang, L., Hu, S., Li, L., Liu, L. and Wan, S., 2014. Decoupling of soil microbes  
662 and plants with increasing anthropogenic nitrogen inputs in a temperate steppe.  
663 *Soil Biology & Biochemistry*, 72: 116-122.

664 Liu, Z., Ma, J., Wei, G., Liu, Q., Jiang, Z., Ding, X., Peng, S., Zeng, T. and Ouyang, T.,  
665 2017. Magnetism of a red soil core derived from basalt, northern Hainan Island,  
666 China: Volcanic ash versus pedogenesis. *Journal of Geophysical Research:*  
667 *Solid Earth*, 122(3): 1677-1696.

668 Lorenz, K. and Lal, R., 2005. The Depth Distribution of Soil Organic Carbon in  
669 Relation to Land Use and Management and the Potential of Carbon  
670 Sequestration in Subsoil Horizons, *Advances in Agronomy*. Academic Press,  
671 88: 35-66.

672 Lu, Y., Si, B., Li, H. and Biswas, A., 2019. Elucidating controls of the variability of  
673 deep soil bulk density. *Geoderma*, 348: 146-157.

674 Luo, Z., Viscarra-Rossel, R.A. and Qian, T., 2021. Similar importance of edaphic and  
675 climatic factors for controlling soil organic carbon stocks of the world.  
676 *Biogeosciences*, 18(6): 2063-2073.

677 Luo, Z., Wang, E. and Sun, O.J., 2010. Soil carbon change and its responses to  
678 agricultural practices in Australian agro-ecosystems: A review and synthesis.



679 Geoderma, 155(3): 211-223.

680 Mathieu, J.A., Hatté, C., Balesdent, J. and Parent, É., 2015. Deep soil carbon dynamics  
681 are driven more by soil type than by climate: a worldwide meta-analysis of  
682 radiocarbon profiles. *Global Change Biology*, 21(11): 4278-4292.

683 Mayer, S., Kühnel, A., Burmeister, J., Kögel-Knabner, I. and Wiesmeier, M., 2019.  
684 Controlling factors of organic carbon stocks in agricultural topsoils and subsoils  
685 of Bavaria. *Soil & Tillage Research*, 192: 22-32.

686 McBride, M.B., 1994. *Environmental Chemistry of Soils*, Oxford University Press,  
687 New York.

688 McGlynn, B.L. and McDonnell, J.J., 2003. Role of discrete landscape units in  
689 controlling catchment dissolved organic carbon dynamics. *Water Resources*  
690 *Research*, 39(4): 1090.

691 Mendiburu, F.d., 2019. *agricolae: Statistical Procedures for Agricultural Research*. R  
692 Package Version 1.3-1: 1-156.

693 Minasny, B., Malone, B.P., McBratney, A.B., Angers, D.A., Arrouays, D., Chambers,  
694 A., Chaplot, V., Chen, Z.-S., Cheng, K., Das, B.S., Field, D.J., Gimona, A.,  
695 Hedley, C.B., Hong, S.Y., Mandal, B., Marchant, B.P., Martin, M., McConkey,  
696 B.G., Mulder, V.L., O'Rourke, S., Richer-de-Forges, A.C., Odeh, I., Padarian,  
697 J., Paustian, K., Pan, G., Poggio, L., Savin, I., Stolbovoy, V., Stockmann, U.,  
698 Sulaeman, Y., Tsui, C.-C., Vågen, T.-G., van Wesemael, B. and Winowiecki,  
699 L., 2017. Soil carbon 4 per mille. *Geoderma*, 292: 59-86.

700 Müller, D., Leitão, P.J. and Sikor, T., 2013. Comparing the determinants of cropland  
701 abandonment in Albania and Romania using boosted regression trees.  
702 *Agricultural Systems*, 117: 66-77.

703 Nelson, D.W. and Sommers, L.E., 1983. Total carbon, organic carbon and organic  
704 matter. *Methods of Soil Analysis: Part 2 Chemical and Microbiological*  
705 *Properties*, 9: 539-579.

706 Niu, X., Liu, C., Jia, X. and Zhu, J., 2021. Changing soil organic carbon with land use  
707 and management practices in a thousand-year cultivation region. *Agriculture,*  
708 *Ecosystems & Environment*, 322: 107639.

709 Orgiazzi, A., Ballabio, C., Panagos, P., Jones, A. and Fernández-Ugalde, O., 2017.  
710 LUCAS Soil, the largest expandable soil dataset for Europe: a review. *European*  
711 *Journal of Soil Science*, 69(1): 140-153.

712 Peng, X., Yan, X., Zhou, H., Zhang, Y. and Sun, H., 2015. Assessing the contributions  
713 of sesquioxides and soil organic matter to aggregation in an Ultisol under long-  
714 term fertilization. *Soil & Tillage Research*, 146: 89-98.

715 Qian, H., Pan, J. and Sun, B., 2013. The relative impact of land use and soil properties  
716 on sizes and turnover rates of soil organic carbon pools in Subtropical China.  
717 *Soil Use and Management*, 29(4): 510-518.

718 R Core Team, 2021. *R: A language and environment for statistical computing*. R  
719 Foundation for Statistical Computing, Vienna, Austria. URL [https://www.R-](https://www.R-project.org/)  
720 [project.org/](https://www.R-project.org/).

721 Richter, D.D. and Babbar, L.I., 1991. Soil Diversity in the Tropics. In: M. Begon, A.H.  
722 Fitter and A. Macfadyen (Editors), *Advances in Ecological Research*. Academic  
723 Press, 21: 315-389.

724 Rizinjirabake, F., Pilesjö, P. and Tenenbaum, D.E., 2019. Dissolved organic carbon  
725 leaching flux in a mixed agriculture and forest watershed in Rwanda. *Journal of*  
726 *Hydrology: Regional Studies*, 26: 100633.

727 Rumpel, C. and Kögel-Knabner, I., 2011. Deep soil organic matter—a key but poorly  
728 understood component of terrestrial C cycle. *Plant & Soil*, 338(1): 143-158.

729 Schlesinger, W.H. and Bernhardt, E.S., 2013. Biogeochemistry: an analysis of global  
730 change. Academic Press, San Diego, California, USA.

731 Schmidt, M.W.I., Torn, M.S., Abiven, S., Dittmar, T., Guggenberger, G., Janssens, I.A.,  
732 Kleber, M., Kogel-Knabner, I., Lehmann, J., Manning, D.A.C., Nannipieri, P.,  
733 Rasse, D.P., Weiner, S. and Trumbore, S.E., 2011. Persistence of soil organic  
734 matter as an ecosystem property. *Nature*, 478(7367): 49-56.

735 Schwanghart, W. and Jarmer, T., 2011. Linking spatial patterns of soil organic carbon  
736 to topography - A case study from south-eastern Spain. *Geomorphology*, 126(1-  
737 2): 252-263.

738 Singh, G., Schoonover, J.E., Williard, K.W.J., Kaur, G. and Crim, J., 2018. Carbon and  
739 nitrogen pools in deep soil horizons at different landscape positions. *Soil  
740 Science Society of America Journal*, 82(6): 1512-1525.

741 Six, J., Conant, R.T., Paul, E.A. and Paustian, K., 2002. Stabilization mechanisms of  
742 soil organic matter: Implications for C-saturation of soils. *Plant & Soil*, 241(2):  
743 155-176.

744 Six, J., Elliott, E.T. and Paustian, K., 2000. Soil macroaggregate turnover and  
745 microaggregate formation: a mechanism for C sequestration under no-tillage  
746 agriculture. *Soil Biology & Biochemistry*, 32(14): 2099-2103.

747 Soil Survey Staff, 2014. Keys to Soil Taxonomy, 12th ed. USDA-Natural Resources  
748 Conservation Service, Washington, DC.

749 Song, X.D., Brus, D.J., Liu, F., Li, D.C., Zhao, Y.G., Yang, J.L. and Zhang, G.L., 2016.  
750 Mapping soil organic carbon content by geographically weighted regression: A  
751 case study in the Heihe River Basin, China. *Geoderma*, 261: 11-22.

752 Song, X.-D., Wu, H.-Y., Liu, F., Tian, J., Cao, Q., Yang, S.-H., Peng, X.-H. and Zhang,  
753 G.-L., 2019. Three-dimensional mapping of organic carbon using piecewise  
754 depth functions in the Red Soil Critical Zone Observatory. *Soil Science Society  
755 of America Journal*, 83(3): 687-696.

756 Sparks, D.L., 2003. *Environmental Soil Chemistry*. Elsevier, San Diego, California,  
757 USA.

758 Spielvogel, S., Prietzel, J. and Kögel-Knabner, I., 2008. Soil organic matter  
759 stabilization in acidic forest soils is preferential and soil type-specific. *European  
760 Journal of Soil Science*, 59(4): 674-692.

761 Sun, H., Wang, Y., Zhao, Y., Zhang, P., Song, Y., He, M., Zhang, C., Tong, Y., Zhou,  
762 J., Qi, L. and Xu, L., 2020. Assessing the value of electrical resistivity derived  
763 soil water content: insights from a case study in the Critical Zone of the Chinese  
764 Loess Plateau. *Journal of Hydrology*: 125132.

765 Tarnocai, C., Canadell, J.G., Schuur, E.A.G., Kuhry, P., Mazhitova, G. and Zimov, S.,  
766 2009. Soil organic carbon pools in the northern circumpolar permafrost region.  
767 *Global Biogeochemical Cycles*, 23(2): GB2023.

768 Tonon, G., Sohi, S., Francioso, O., Ferrari, E., Montecchio, D., Gioacchini, P., Ciavatta,  
769 C., Panzacchi, P. and Powlson, D., 2010. Effect of soil pH on the chemical  
770 composition of organic matter in physically separated soil fractions in two  
771 broadleaf woodland sites at Rothamsted, UK. *European Journal of Soil Science*,  
772 61(6): 970-979.

773 Trumbore, S., 2009. Radiocarbon and Soil Carbon Dynamics. *Annual Review of Earth  
774 and Planetary Sciences*, 37(1): 47-66.

775 Wade, A.M., Richter, D.D., Medjibe, V.P., Bacon, A.R., Heine, P.R., White, L.J.T. and  
776 Poulsen, J.R., 2019. Estimates and determinants of stocks of deep soil carbon in  
777 Gabon, Central Africa. *Geoderma*, 341: 236-248.

778 Wang, S., Zhuang, Q., Wang, Q., Jin, X. and Han, C., 2017. Mapping stocks of soil

779 organic carbon and soil total nitrogen in Liaoning Province of China. *Geoderma*,  
780 305: 250-263.

781 Wang, Y., Han, X., Jin, Z., Zhang, C. and Fang, L., 2016. Soil organic carbon stocks in  
782 deep soils at a watershed scale on the Chinese Loess Plateau. *Soil Science*  
783 *Society of America Journal*, 80(1): 157-167.

784 Wang, Y., Shao, M.a., Zhang, C., Liu, Z., Zou, J. and Xiao, J., 2015. Soil organic carbon  
785 in deep profiles under Chinese continental monsoon climate and its relations  
786 with land uses. *Ecological Engineering*, 82: 361-367.

787 Wickham, H., 2016. *ggplot2: Elegant graphics for data analysis*. Springer.

788 Wilson, M., He, Z. and Yang, X., 2004. *The red soils of China: their nature,*  
789 *management and utilization*. Springer Science & Business Media.

790 Wu, H., Song, X., Zhao, X., Peng, X., Zhou, H., Hallett, P.D., Hodson, M.E. and Zhang,  
791 G.-L., 2019a. Accumulation of nitrate and dissolved organic nitrogen at depth  
792 in a red soil Critical Zone. *Geoderma*, 337: 1175-1185.

793 Wu, H.Y., Adams, J.M., Shi, Y., Li, Y.T., Song, X.D., Zhao, X.R., Chu, H.Y. and  
794 Zhang, G.L., 2019b. Depth-Dependent Patterns of Bacterial Communities and  
795 Assembly Processes in a Typical Red Soil Critical Zone. *Geomicrobiology*  
796 *Journal*, 37(3): 201-212.

797 Xu, X., Shi, Z., Li, D., Rey, A., Ruan, H., Craine, J.M., Liang, J., Zhou, J. and Luo, Y.,  
798 2016. Soil properties control decomposition of soil organic carbon: Results from  
799 data-assimilation analysis. *Geoderma*, 262: 235-242.

800 Yang, F., Zhang, G.L., Yang, J.L., Li, D.C., Zhao, Y.G., Liu, F., Yang, R.M. and Yang,  
801 F., 2014. Organic matter controls of soil water retention in an alpine grassland  
802 and its significance for hydrological processes. *Journal of Hydrology*, 519:  
803 3086-3093.

804 Yang, L., Wei, W., Chen, L. and Mo, B., 2012. Response of deep soil moisture to land  
805 use and afforestation in the semi-arid Loess Plateau, China. *Journal of*  
806 *Hydrology*, 475: 111-122.

807 Yang, M., Wang, S., Zhao, X., Gao, X. and Liu, S., 2020a. Soil properties of apple  
808 orchards on China's Loess Plateau. *Science of The Total Environment*, 723:  
809 138041.

810 Yang, S., Wu, H., Dong, Y., Zhao, X., Song, X., Yang, J., Hallett, P.D. and Zhang, G.-  
811 L., 2020c. Deep nitrate accumulation in a highly weathered subtropical Critical  
812 Zone depends on the regolith structure and planting year. *Environmental*  
813 *Science & Technology*, 54(21): 13739-13747.

814 Yang, S.-H., Wu, H.-Y., Song, X.-D., Dong, Y., Zhao, X.-R., Cao, Q., Yang, J.-L. and  
815 Zhang, G.-L., 2020b. Variation of deep nitrate in a typical red soil Critical Zone:  
816 Effects of land use and slope position. *Agriculture, Ecosystems & Environment*,  
817 297: 106966.

818 Yao, X., Yu, K., Deng, Y., Zeng, Q., Lai, Z. and Liu, J., 2019. Spatial distribution of  
819 soil organic carbon stocks in Masson pine (*Pinus massoniana*) forests in  
820 subtropical China. *CATENA*, 178: 189-198.

821 Yu, H., Zha, T., Zhang, X. and Ma, L., 2019a. Vertical distribution and influencing  
822 factors of soil organic carbon in the Loess Plateau, China. *Science of The Total*  
823 *Environment*, 693: 133632.

824 Yu, H., Zha, T., Zhang, X., Nie, L., Ma, L. and Pan, Y., 2020a. Spatial distribution of  
825 soil organic carbon may be predominantly regulated by topography in a small  
826 revegetated watershed. *CATENA*, 188: 104459.

827 Yu, X., Zhou, W., Chen, Y., Wang, Y., Cheng, P., Hou, Y., Wang, Y., Xiong, X. and  
828 Yang, L., 2019b. Spatial variation of soil properties and carbon under different

829 land use types on the Chinese Loess Plateau. *Science of The Total Environment*,  
830 703: 134946.

831 Yu, X., Zhou, W., Wang, Y., Cheng, P., Hou, Y., Xiong, X., Du, H., Yang, L. and Wang,  
832 Y., 2020b. Effects of land use and cultivation time on soil organic and inorganic  
833 carbon storage in deep soils. *Journal of Geographical Sciences*, 30(6): 921-934.

834 Zhang, G., Zhu, Y. and Shao, M.a., 2019. Understanding sustainability of soil and water  
835 resources in a critical zone perspective. *Science China Earth Sciences*, 62:  
836 1716–1718.

837 Zhang, G.L. and Gong, Z.T., 2012. *Soil Survey Laboratory Methods*. Science Press (In  
838 Chinese), Beijing.

839 Zhang, M. and He, Z., 2004. Long-term changes in organic carbon and nutrients of an  
840 Ultisol under rice cropping in southeast China. *Geoderma*, 118(3): 167-179.

841 Zhang, M.K. and Xu, J.M., 2005. Restoration of surface soil fertility of an eroded red  
842 soil in southern China. *Soil & Tillage Research*, 80(1): 13-21.

843 Zhang, X., Guo, J., Vogt, R.D., Mulder, J., Wang, Y., Qian, C., Wang, J. and Zhang,  
844 X., 2020. Soil acidification as an additional driver to organic carbon  
845 accumulation in major Chinese croplands. *Geoderma*, 366: 114234.

846 Zhang, Z., Yu, D., Shi, X., Warner, E., Ren, H., Sun, W., Tan, M. and Wang, H., 2010.  
847 Application of categorical information in the spatial prediction of soil organic  
848 carbon in the red soil area of China. *Soil Science & Plant Nutrition*, 56(2): 307-  
849 318.

850 Zhao, X.-R., Wu, H.-Y., Song, X.-D., Yang, S.-H., Dong, Y., Yang, J.-L. and Zhang,  
851 G.-L., 2019. Intra-horizon differentiation of the bacterial community and its co-  
852 occurrence network in a typical Plinthic horizon. *Science of The Total  
853 Environment*, 678: 692-701.

854 Zhao, Y., Wang, M., Hu, S., Zhang, X., Ouyang, Z., Zhang, G., Huang, B., Zhao, S.,  
855 Wu, J. and Xie, D., 2018. Economics-and policy-driven organic carbon input  
856 enhancement dominates soil organic carbon accumulation in Chinese croplands.  
857 *Proceedings of the National Academy of Sciences*, 115(16): 4045-4050.

858 Zhou, Y., Hartemink, A.E., Shi, Z., Liang, Z. and Lu, Y., 2019. Land use and climate  
859 change effects on soil organic carbon in North and Northeast China. *Science of  
860 The Total Environment*, 647: 1230-1238.

861 Zhu, H., Wu, J., Huang, D., Zhu, Q., Liu, S., Su, Y., Wei, W., Syers, J.K. and Li, Y.,  
862 2010. Improving fertility and productivity of a highly-weathered upland soil in  
863 subtropical China by incorporating rice straw. *Plant & Soil*, 331(1): 427-437.

864 **Table and Figure Captions**

865 **Table 1.** Means and standard deviations (in brackets) of total organic carbon stocks  
866 (Mg C ha<sup>-1</sup>) at different depth intervals.

867 **Figure 1** Global distribution of red soil (referenced as Oxisols and Ultisols) (a) derived  
868 from Eswaran et al. (2012). Location of the study area in China (b). Spatial distribution  
869 of the 21 boreholes with an aerial base map (c). Numbers affiliated are drilling order  
870 during the field investigation.

871 **Figure 2** Vertical distribution of TOC content from land surface to bedrock for the 21  
872 drilling boreholes. The data for W3 between 1050 and 1950 cm was not shown for  
873 clarity.

874 **Figure 3** Vertical distribution of cumulative TOC stock and proportion from land  
875 surface to bedrock for the 21 drilling boreholes. The data for W3 between 1050 and  
876 1950 cm was not shown for clarity.

877 **Figure 4** Relative importance of regolith properties (pH, silt, clay, sand, BD and WC)  
878 of the BRT models. Data are from depths 0 cm – bedrock, 0-100 cm and 100 cm -  
879 bedrock respectively. TOC, total organic carbon stock; BD, bulk density; WC, water  
880 content. The black line represents the cumulative TOC stock with increasing depth,  
881 while the blue line indicates the cumulative proportion of TOC with increasing depth.

882 **Figure 5** Vertical distribution of TOC under different land use types at different depth  
883 intervals. Different lowercase letters (a and b) indicate that values were significantly  
884 different in the same land use ( $p < 0.05$ ).

885 **Figure 6** The distribution of mean TOC stock for different land uses at four depths.

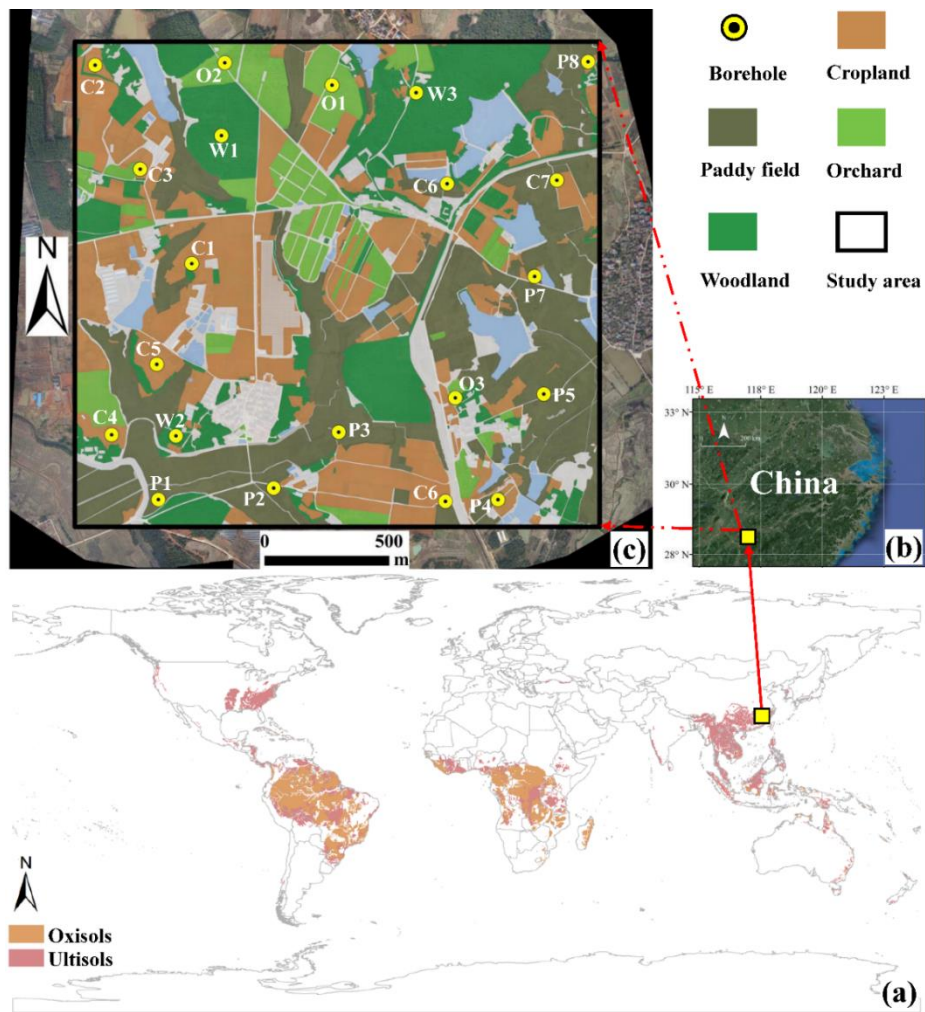
886 Different lowercase letters (a, b and c) indicate that values were significantly different  
887 in the same land use ( $p < 0.05$ ). Different uppercase letters (A, B and C) indicate that  
888 values were significantly different at the same depth ( $p < 0.05$ ). The error bars indicate  
889 the standard error. n is the number of sample sites.

890 **Figure 7** The distribution of mean TOC stock for different land uses at four depths.  
891 Different lowercase letters (a, b and c) indicate that values were significantly different  
892 in the same land use ( $p < 0.05$ ). Different uppercase letters (A, B and C) indicate that  
893 values were significantly different at the same depth ( $p < 0.05$ ). The error bars indicate  
894 the standard error. n is the number of sample sites.

895 **Table 1.** Means and standard deviations (in brackets) of TOC stocks (Mg C ha<sup>-1</sup>) at  
 896 different depth intervals.

Depth (cm)	Paddy field (n=8)	Cropland (n=7)	Woodland (n=3)	Orchard (n=3)	Total (n=21)
0-30 cm	44.2 (9.0)	21.4 (4.2)	23.9 (7.1)	17.9 (5.1)	23.0 (13.3)
30-100 cm	35.3 (8.4)	19.9 (3.1)	21.5 (2.2)	29.4 (9.7)	27.3 (9.4)
0-100 cm	79.5 (16.0)	41.2 (5.3)	45.4 (9.2)	47.3 (6.6)	57.3 (20.9)
100 cm-bedrock	111.5 (53.2)	113.2 (55.0)	125.2 (73.3)	90.8 (44.3)	111.1 (52.2)

897



898

899 **Figure 1** Global distribution of red soil (referenced as Oxisols and Ultisols) (a) derived  
 900 from Eswaran et al. (2012). Location of the study area in China (b). Spatial distribution  
 901 of the 21 boreholes with an aerial base map (c). Numbers affiliated are drilling order  
 902 during the field investigation.





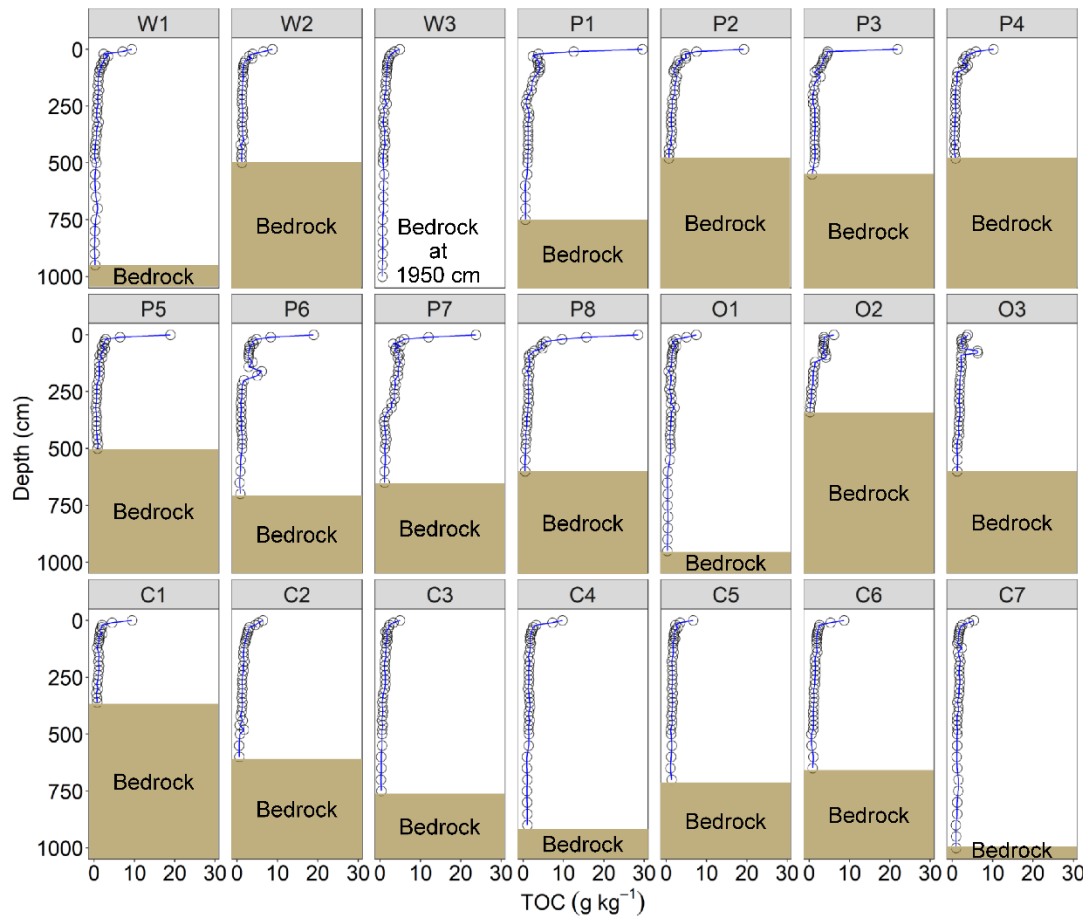
903

904 **Figure 2** Borehole drilling in the field (a). Regolith core obtained by the drill (b).

905 Observation and measurement of regolith core (c). Soil adhering to the inner wall of

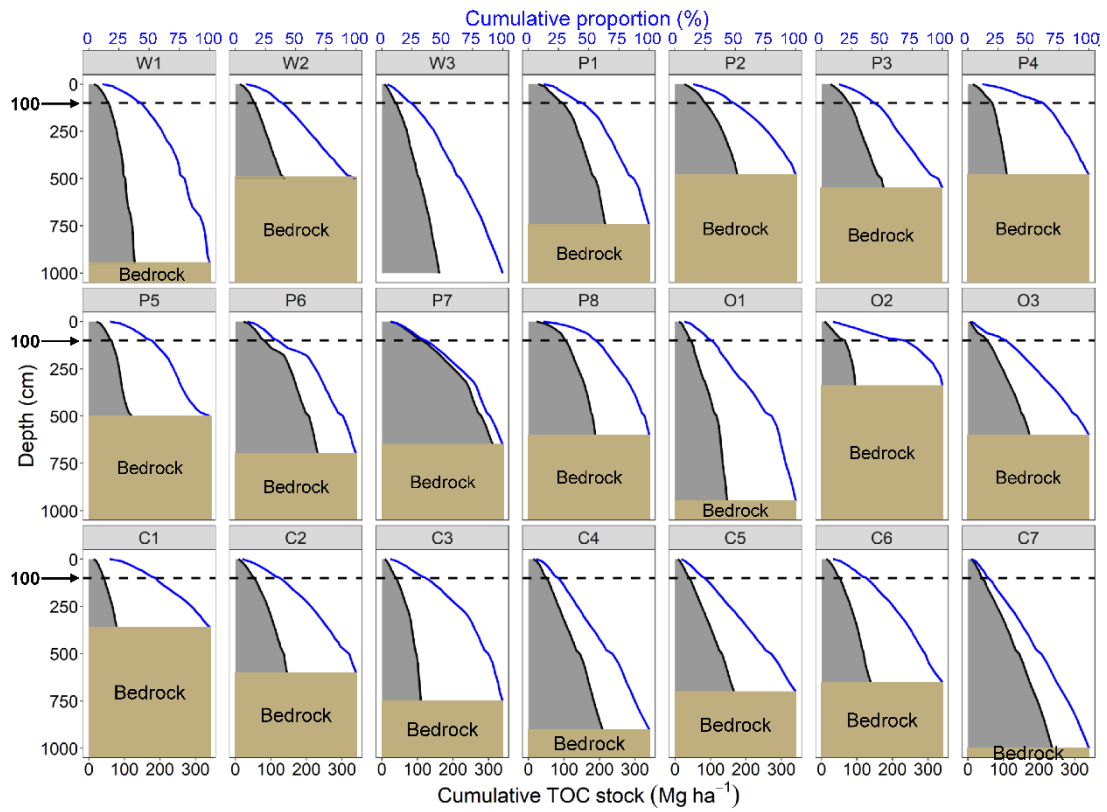
906 cylinder was cut and discarded to avoid potential contamination (d). Regolith core used

907 to sample (e). Sampling strategy at different depth intervals (f).



908

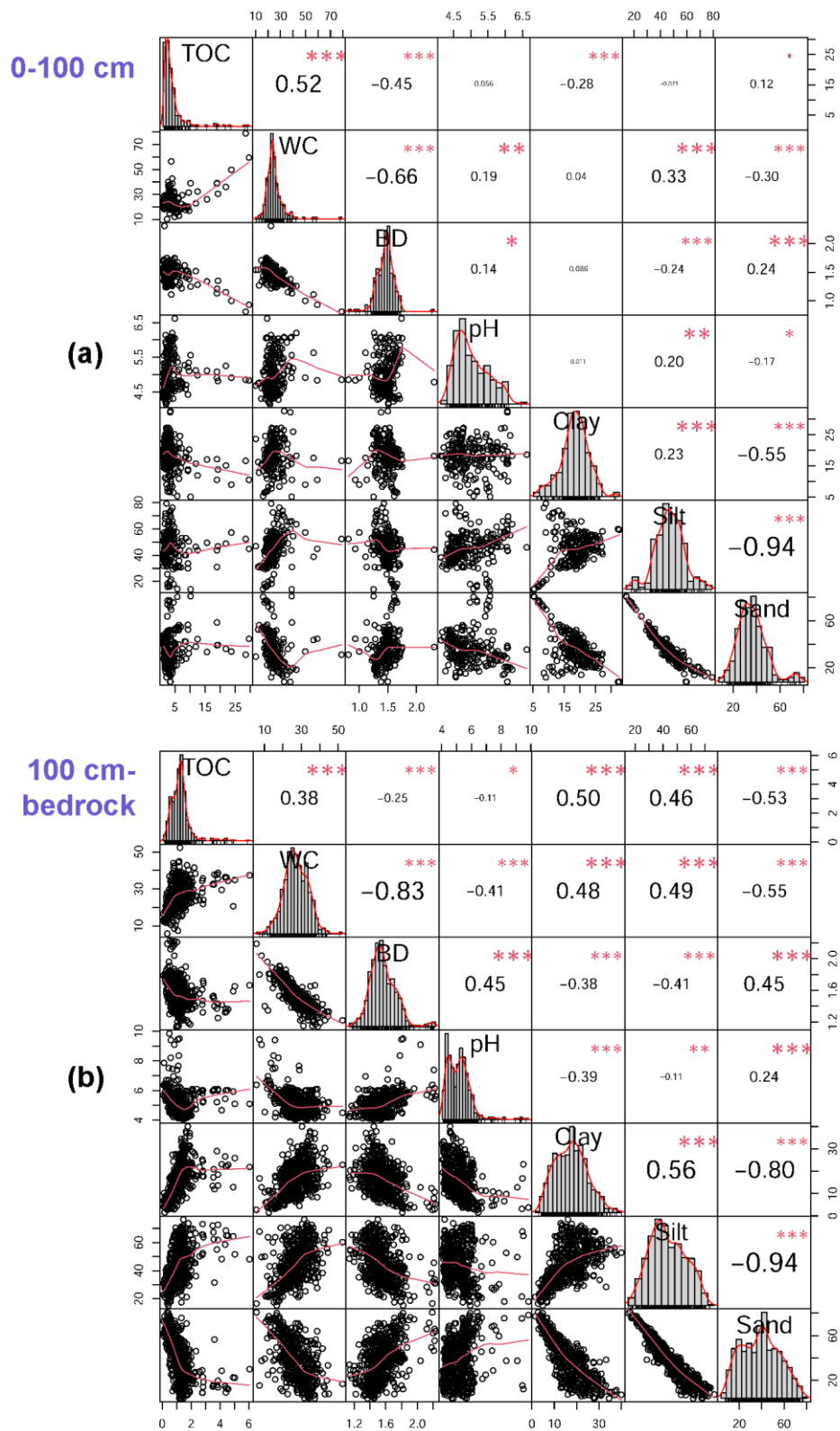
909 **Figure 3** Vertical distribution of TOC content from land surface to bedrock for the 21  
 910 drilling boreholes. The data for W3 between 1050 and 1950 cm was not shown for  
 911 clarity.



912

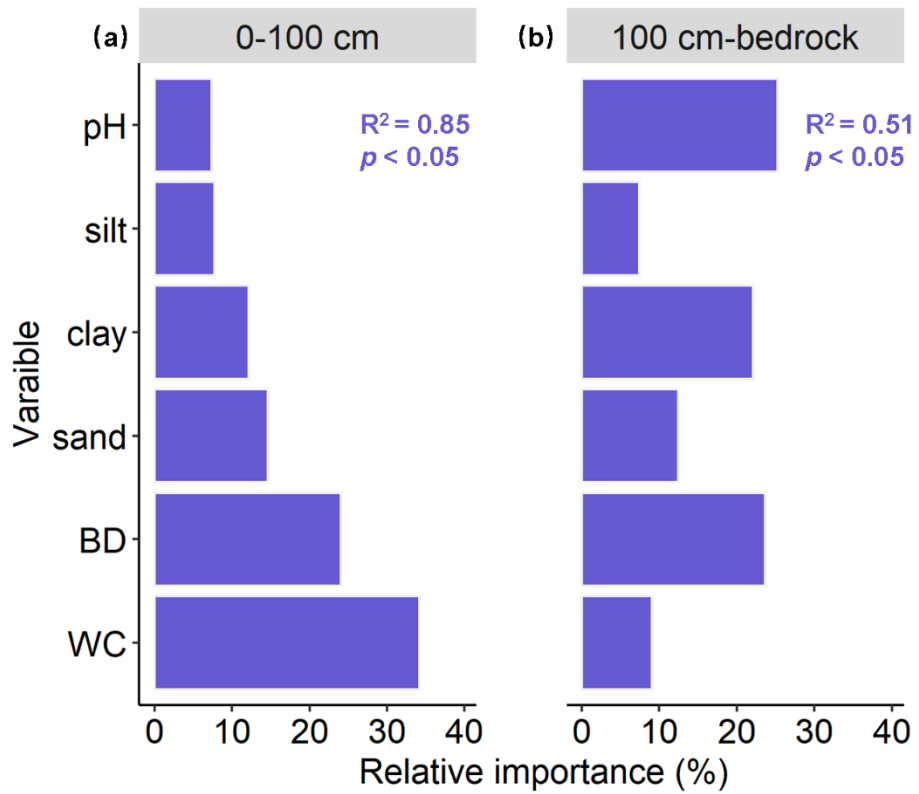
913 **Figure 4** Vertical distribution of cumulative TOC stock and proportion from land  
 914 surface to bedrock for the 21 drilling boreholes. The data for W3 between 1050 and  
 915 1950 cm was not shown for clarity. The black line represents the cumulative TOC stock  
 916 with increasing depth, while the blue line indicates the cumulative proportion of TOC  
 917 with increasing depth.

918



919

920 **Figure 5** Pearson correlation between total organic carbon (TOC) and selected edaphic  
 921 factors for the depths of 0-100 cm and 100 cm-bedrock, respectively. \*,  $p < 0.05$ ; \*\*,  $p$   
 922  $< 0.01$ ; \*\*\*,  $p < 0.001$ .

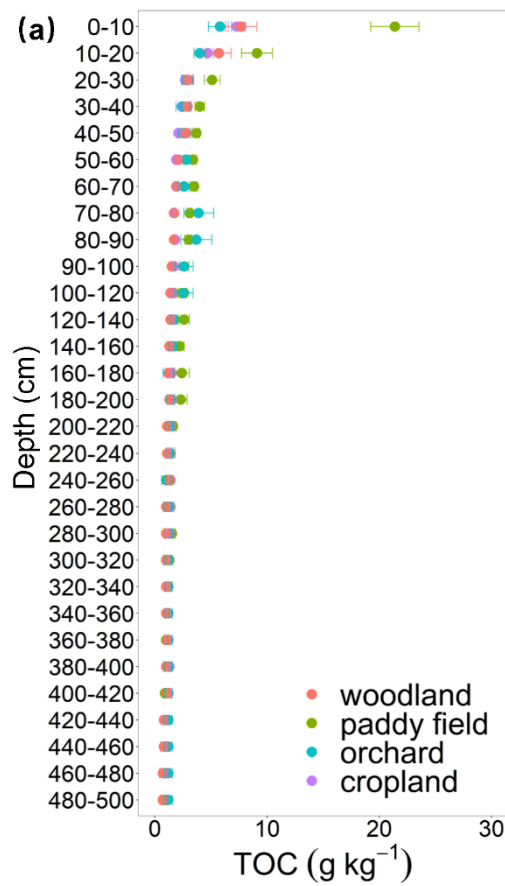


923

924 **Figure 6** Relative importance of regolith properties (pH, silt, clay, sand, BD and WC)

925 of the BRT models. Data are from depths 0-100 cm and 100 cm - bedrock respectively.

926 TOC, total organic carbon stock; BD, bulk density; WC, water content.

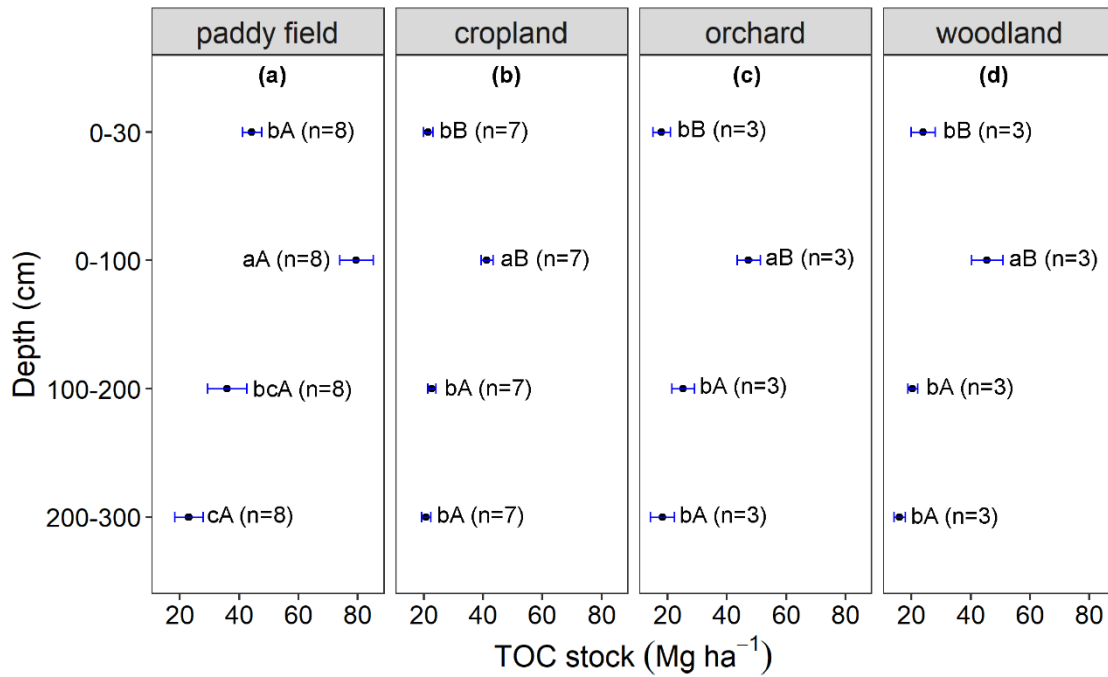


(b)

Depth (cm)	W	P	O	C
0-10	b	a	b	b
10-20	ab	a	b	b
20-30	b	a	b	b
30-40	ab	a	b	b
40-50	ab	a	b	b
50-60	b	a	ab	b
60-70	b	a	b	b
70-80	b	a	a	b
80-90	b	a	a	b
90-100	a	a	a	a
100-120	a	a	a	a
120-140	a	a	a	a
140-160	a	a	a	a
160-180	a	a	a	a
180-200	a	a	a	a
200-220	a	a	a	a
220-240	a	a	a	a
240-260	a	a	a	a
260-280	a	a	a	a
280-300	a	a	a	a
300-320	a	a	a	a
320-340	a	a	a	a
340-360	a	a	a	a
360-380	a	a	a	a
380-400	a	a	a	a
400-420	a	a	a	a
420-440	a	a	a	a
440-460	a	a	a	a
460-480	a	a	a	a
480-500	a	a	a	a

927

928 **Figure 7** Vertical distribution of TOC under different land use types at different depth  
 929 intervals. Different lowercase letters (a and b) indicate that values were significantly  
 930 different in the same land use ( $p < 0.05$ ).



931

932 **Figure 8** The distribution of mean TOC stock for different land uses at four depths.

933 Different lowercase letters (a, b and c) indicate that values were significantly different

934 in the same land use ( $p < 0.05$ ). Different uppercase letters (A, B and C) indicate that

935 values were significantly different at the same depth ( $p < 0.05$ ). The error bars indicate

936 the standard error. n is the number of sample sites.